

2021-09-27

# Ozone and nitrogen dioxide pollution in a coastal urban environment: the role of ...

*This work was made openly accessible by BU Faculty. Please [share](#) how this access benefits you. Your story matters.*

Version	Published version
Citation (published version):	J.A. Geddes, B. Wang, D. Li. 2021. "Ozone and Nitrogen Dioxide Pollution in a Coastal Urban Environment: The Role of Sea Breezes, and Implications of Their Representation for Remote Sensing of Local Air Quality." <i>Journal of Geophysical Research: Atmospheres</i> , Volume 126, Issue 18, pp.e2021JD035314-. <a href="https://doi.org/10.1029/2021JD035314">https://doi.org/10.1029/2021JD035314</a>

<https://hdl.handle.net/2144/46465>

*Boston University*



## RESEARCH ARTICLE

10.1029/2021JD035314

### Key Points:

- Sea breezes play a distinct role in the distribution of primary and secondary pollution throughout the urban Boston area
- Steep spatial gradients in secondary pollution occur during sea breezes, posing a challenge to traditional air monitoring networks
- The sea breeze also presents unique challenges in long-term averages of air quality derived from satellite instruments

### Supporting Information:

Supporting Information may be found in the online version of this article.

### Correspondence to:

J. A. Geddes,  
[jgeddes@bu.edu](mailto:jgeddes@bu.edu)

### Citation:

Geddes, J. A., Wang, B., & Li, D. (2021). Ozone and nitrogen dioxide pollution in a coastal urban environment: The role of sea breezes, and implications of their representation for remote sensing of local air quality. *Journal of Geophysical Research: Atmospheres*, 126, e2021JD035314. <https://doi.org/10.1029/2021JD035314>

Received 25 MAY 2021

Accepted 25 AUG 2021

### Author Contributions:

**Conceptualization:** Jeffrey A. Geddes

**Formal analysis:** Jeffrey A. Geddes

**Funding acquisition:** Jeffrey A. Geddes

**Investigation:** Bo Wang

**Methodology:** Jeffrey A. Geddes, Bo Wang, Dan Li

**Project Administration:** Jeffrey A. Geddes

**Resources:** Bo Wang

**Visualization:** Jeffrey A. Geddes

© 2021. The Authors.

This is an open access article under the terms of the [Creative Commons Attribution-NonCommercial-NoDerivs License](https://creativecommons.org/licenses/by/4.0/), which permits use and distribution in any medium, provided the original work is properly cited, the use is non-commercial and no modifications or adaptations are made.

# Ozone and Nitrogen Dioxide Pollution in a Coastal Urban Environment: The Role of Sea Breezes, and Implications of Their Representation for Remote Sensing of Local Air Quality

Jeffrey A. Geddes<sup>1</sup> , Bo Wang<sup>1</sup>, and Dan Li<sup>1</sup> 

<sup>1</sup>Department of Earth & Environment, Boston University, Boston, MA, USA

**Abstract** We present an analysis of sea breeze conditions for the Boston region and examine their impact on the concentration of local air pollutants over the past decade. Sea breezes occur about one-third of the days during the summer and play an important role in the spatial distribution and temporal evolution of NO<sub>2</sub> and O<sub>3</sub> across the urban area. Mornings preceding a sea breeze are characterized by low horizontal wind speeds, low background O<sub>3</sub>, and an accumulation of local primary emissions. Air pollution is recirculated inland during sea breezes, frequently coinciding with the highest O<sub>3</sub> measured at the urban center. We use “Ox” (= NO<sub>2</sub> + O<sub>3</sub>) to account for temporary O<sub>3</sub> suppression by NO and find large horizontal gradients (differences in Ox greater than 30 ppb across less than 15 km), which are not observed on otherwise westerly or easterly prevailing days. This implies a challenge in surface monitoring networks to adequately represent the spatial variability of secondary air pollution in coastal urban areas. We investigate satellite-based climatologies of tropospheric NO<sub>2</sub>, and find evidence of selection biases due to cloud conditions, but show that sea breeze days are well observed due to the fair weather conditions generally associated with these events. The fine scale of the sea breeze in Boston is not reliably represented by meteorological reanalyses products commonly used in chemical transport models required to provide inputs for the satellite-based retrievals. This implies a higher systematic error in the operational retrievals on sea breeze days compared to other days.

**Plain Language Summary** Coastal areas experience unique small-scale weather systems called sea breezes where winds at the surface blow from the land to the ocean in the morning, then reverse to blow from the ocean toward the land in the afternoon. These systems can affect the distribution of air pollution in coastal urban environments. In the case of the Boston area, we find that sea breezes result in the accumulation of local air pollutant emissions in the morning, and cause a rapid buildup of pollution during the afternoon as the air is recirculated back inland, even though those days tend to start with lower background pollution conditions. The breeze systems also cause large spatial variability in the pollution that is not observed on the days when winds are continuously blowing from west or east all day. We also show that while satellite observations of air quality can generally capture the expected behavior of pollution distribution at the surface, there are difficulties in the interpretation and accuracy of these products over the long term due to cloud cover variability and the small spatial scale in the wind patterns of a sea breeze.

## 1. Introduction

Despite comprising less than 10% of the land area in the contiguous US, almost 40% of the country’s population lives in coastal shoreline counties (NOAA, 2021). In addition to being vulnerable to a host of environmental risks (e.g., flooding, hurricanes, sea level rise, and erosion), these regions experience unique meteorological phenomena that are specific to coastlines, and which can strongly influence the distribution of air pollution within coastal cities. Quantifying the distribution of atmospheric constituents that impact human health, and understanding the influence of meteorological processes on this distribution, remain priority research areas in atmospheric chemistry (NAS, 2016).

The “sea breeze” (and its “lake breeze” counterpart) is a prominent example of a meteorological process unique to coastal regions that can influence the distribution of trace atmospheric species. At its simplest,

**Writing – original draft:** Jeffrey A. Geddes

**Writing – review & editing:** Jeffrey A. Geddes, Bo Wang, Dan Li

this phenomenon results from the more rapid heating of land surfaces than the ocean surface during the day, causing thermal contrast that creates a local pressure gradient force characterized by onshore air flow at the surface. These systems can be characterized by a sea breeze front, demarcating potentially steep gradients in air temperature, moisture, and winds. A detailed review of our understanding of sea breeze circulations is provided for example by Miller (2003). The forcing, structure, and life cycle of sea breeze circulations, and their interactions with larger-scale (synoptic) meteorological systems, are highly variable.

The role of these circulation systems on the distribution of air pollution and atmospheric chemistry in coastal urban environments continues to be explored in recent case studies, field campaigns, and long-term observational analyses [e.g., in the mid-Atlantic US (Loughner et al., 2014; Mazzuca et al., 2019; Stauffer & Thompson, 2015), Los Angeles (Wagner et al., 2012), Houston (Caicedo et al., 2019), Salt Lake City (Blaylock et al., 2017), Lake Michigan (Vermeuel et al., 2019), and Lake Ontario (Wentworth et al., 2015), and elsewhere around the world including around the Mediterranean (Castell et al., 2008; Finardi et al., 2018; Mavrakou et al., 2012), and in East Asia (Hwang et al., 2007; Lin et al., 2007; H. Wang et al., 2018; L. Zhang et al., 2017)]. These studies often demonstrate the capacity of sea breezes to worsen air pollution at the surface. For example, Stauffer and Thompson (2015) demonstrate that bay breezes in the Chesapeake Bay generally exacerbate air quality problems there and that the fraction of ground-level O<sub>3</sub> exceedances occurring on bay breeze days has increased over time at certain locations. Likewise, Wentworth et al. (2015) and Lennartson and Schwartz (2002) show that O<sub>3</sub> exceedance days in Toronto and eastern Wisconsin, respectively, occur either exclusively or at least disproportionately on lake breeze-influenced days.

The role of mesoscale circulation, including sea breezes, on O<sub>3</sub> concentrations around New England specifically has also been studied in some previous work. Mao and Talbot (2004) postulated that the sea breeze in this region may play a minimal role on O<sub>3</sub> concentrations inland during high O<sub>3</sub> episodes, due to the dominance of synoptic southwesterly flow, but that it could explain steep gradients in O<sub>3</sub> concentrations between inland, coastal, and marine sites. Angevine et al. (2004) and Darby et al. (2007) showed that sea breeze circulations can modify the transport of polluted air from the Boston region, bringing O<sub>3</sub>-rich air inland along the New Hampshire coast. However, none of this previous work focused on the role of sea breezes on the distribution of pollution within the most populated areas of the region and the city of Boston itself.

Common in several studies is the observation of stagnant conditions on breeze days, resulting in the accumulation of local primary emissions (Caicedo et al., 2019; Loughner et al., 2014; Stauffer & Thompson, 2015; Wentworth et al., 2015). On the other hand, specific mechanisms for enhanced secondary pollution may involve a number of processes that vary regionally, for example, lower boundary layer mixing heights, reduced deposition over the lake/ocean before air is recirculated over land, more active photochemistry involving the accumulation of precursors, or subsidence of O<sub>3</sub>-rich air from aloft in the return flow of the circulation system. Whatever the case may be, O<sub>3</sub> mixing ratios have been shown to vary by 30 ppb or more between sites within versus immediately outside of the breeze circulation system (e.g., Blaylock et al., 2017; Mao & Talbot, 2004; Vermeuel et al., 2019; Wentworth et al., 2015), implying strong gradients in secondary pollution over relatively short distances in coastal urban environments during these events.

Satellite observations of tropospheric NO<sub>2</sub> abundance have the potential to provide further insight into the distribution of primary pollutant emissions, with important applications in air quality management (e.g., Duncan et al., 2014). Long-term records from the OMI instrument, for example, have helped identify remarkable trends in NO<sub>2</sub> around the world (e.g., Duncan et al., 2016; Krotkov et al., 2016). The more recently launched TROPOMI instrument provides the best spatial resolution that has been achieved for NO<sub>2</sub>, with daily overpasses characterized by  $\sim 3.5 \times 5.5$  km footprints (Eskes et al., 2020; Veefkind et al., 2012). This spatial scale is sufficient to capture individual point sources and estimate emissions from urban areas on specific days (Goldberg et al., 2019), but to gain insight into air quality near the surface these observations must be retrieved during clear sky conditions. This selection process could impart selection biases in long-term averages (Geddes et al., 2012). Moreover, even under the most ideal observing conditions (e.g., clear skies with minimal aerosol loading), large differences between ground-based and satellite-based observations have been noted (e.g., Reed et al., 2015). Disagreements are expected due to differences in the spatial area represented by ground-based and satellite-based instruments (e.g., Kharol et al., 2015), but it has also been well established that the satellite-derived quantity is affected by the spatial and temporal resolution of the geophysical and chemical inputs required in the retrieval (Goldberg et al., 2017; Laughner et al., 2016;

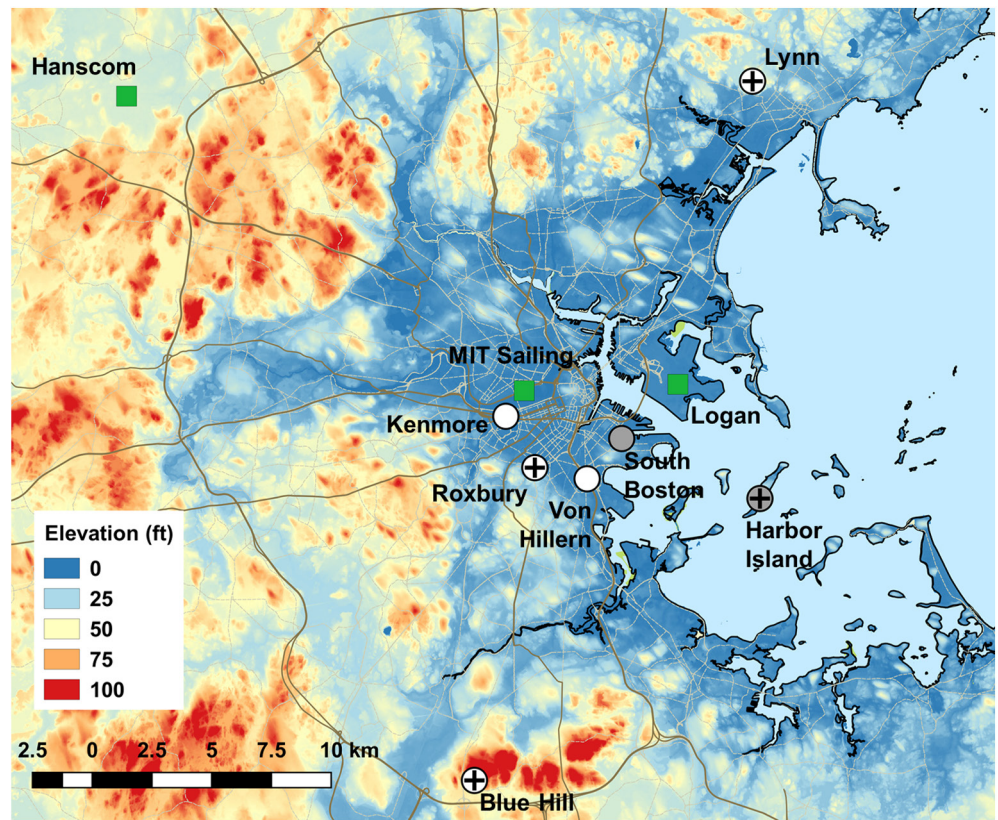


**Figure 1.** Topographical map of the Boston basin, showing MassDEP air monitoring sites (circles) and auxiliary meteorological observations (squares). Circles denote the NO<sub>2</sub> monitoring sites and a “+” symbol denotes sites with collocated O<sub>3</sub> observations. Gray markers denote sites that were active until 2013 (South Boston) and 2014 (Harbor Island); all other locations remain currently active (as of 2019).

Russell et al., 2011; Valin et al., 2011). The potential uncertainties related to these inputs during sea breeze events specifically have not been investigated in detail.

Here, we present the first climatological analysis of O<sub>3</sub> and NO<sub>2</sub> surface concentrations across the greater Boston area and document the impacts of sea breezes on the distribution of these pollutants. While air quality in Boston has improved substantially in recent decades, it remains on the cusp of violating the Environmental Protection Agency’s air quality standard for O<sub>3</sub>, and there has never been a systematic investigation of the role of sea breezes on O<sub>3</sub> and its precursors in this urban area. We document the frequency of sea breezes and describe their conditions in detail. We contrast pollutant concentrations and spatial gradients during sea breeze conditions with those during other meteorological conditions that prevail in the region. This long-term perspective provides insight into the challenge of designing surface monitoring networks that adequately capture pollutant variability in coastal urban areas. We also explore satellite remote sensing of NO<sub>2</sub> during the sea breeze, and test hypotheses about statistical sampling and meteorological biases in these satellite retrievals, to highlight the difficulty of applying these products in such locally complex situations. Our results have implications for characterizing ground-level air quality in coastal urban areas by both in-situ and satellite remote sensing techniques.

## 2. Data and Methods

### 2.1. Surface Monitoring of O<sub>3</sub> and NO<sub>2</sub>

Ground-based observations of O<sub>3</sub> and NO<sub>2</sub> are collected and reported by the Massachusetts Department of Environmental Protection (MassDEP). The locations of these monitoring sites are shown in Figure 1.

Following quality control and quality assurance, these data are reported to the EPA and made publicly available through the AQS repository at: [https://aqs.epa.gov/aqsweb/airdata/download\\_files.html](https://aqs.epa.gov/aqsweb/airdata/download_files.html).

Ambient NO<sub>2</sub> is measured using a technique based on the conversion of NO<sub>2</sub> to NO by a heated molybdenum catalyst followed by a reaction with O<sub>3</sub> which produces a chemiluminescence signal that is proportional to the original NO<sub>2</sub> concentrations. This technique is not selective and is known to suffer from interferences by certain other oxides of nitrogen that can contribute to the NO<sub>2</sub> measurement (Dunlea et al., 2007; Steinbacher et al., 2007). This issue is expected to be the least problematic at urban sites where the majority of total oxides of nitrogen will be made up of NO and NO<sub>2</sub>. We do not expect interference to affect the conclusions of this study since the measurements are a reliable proxy for NO<sub>2</sub> and our results are not dependent on absolute concentrations. Ambient O<sub>3</sub> is measured using a technique based on UV photometry, where O<sub>3</sub> absorption of UV light is recorded at 254 nm, and the amount of absorption is directly proportional to O<sub>3</sub> concentrations. Further details on the MassDEP air quality monitoring network can be found at <https://www.mass.gov/air-monitoring-in-massachusetts>.

## 2.2. Surface Meteorological Observations

Surface meteorological observations in the region are publicly available from the NOAA ISD Lite database (<ftp://ftp.ncdc.noaa.gov/pub/data/noaa/isd-lite/>). We use air temperature, wind speed, and wind direction available from three locations in Eastern Massachusetts (Logan Airport, Hanscom Air Force Base, and Blue Hill). Meteorological observations from a fourth location (the MIT Sailing Pavilion) are reported at <https://sailing.mit.edu/weather/>, an archive of which was made available by request to the website administrator. The locations of these four weather stations are shown in Figure 1.

## 2.3. Aircraft Meteorological Data Reports

We use Aircraft Meteorological Data Reports (AMDAR) for Logan Airport, archived and publicly available from the Meteorological Assimilation Data Ingest System at <https://madis-data.cprk.ncep.noaa.gov/madisPublic1/data/archive/>. We make use of a secondary data product reporting hourly profiles of wind and potential temperature at 20-m vertical resolution, documented by Zhang et al. (2019) and publicly available at <https://zenodo.org/record/3934378#.YGsWUa9Kg2z>. This product merges all raw AMDAR observations within an hour into a single profile interpolated onto a regular grid. Data below 1,500 m that is more than 15 km away from the airport are removed to reduce the influence of horizontal variations within the boundary layer. For robustness, the product further requires at least 10 measurements within the first 1,500 m to be included in the hourly product.

## 2.4. Meteorological Reanalysis and Analysis Data Products

We make use of several atmospheric reanalysis and analysis products. The Modern-Era Retrospective analysis for Research and Applications Version 2 (“MERRA-2”) is an atmospheric reanalysis produced by the Global Modeling and Assimilation Office (GMAO) at NASA. MERRA-2 is provided at 0.5° × 0.625° horizontal resolution and 72 vertical layers and is documented in detail by Gelaro et al. (2017). The North American Regional Reanalysis (NARR) is an atmospheric reanalysis produced by the National Centers for Environmental Prediction (NCEP) at NOAA. NARR is provided at 32 km horizontal resolution and 29 vertical levels and is documented in detail by Mesinger et al. (2006). The MERRA-2 and NARR products are available publicly from <https://disc.gsfc.nasa.gov/> and <https://ncdc.noaa.gov/> respectively. We also make use of the North American Mesoscale (NAM) historical analysis product. The NAM data is produced by NCEP using the WRF Non-hydrostatic Mesoscale Model (Janjic et al., 2001), is available over the continental US at 12 km horizontal resolution, and is described in more detail at [https://www.emc.ncep.noaa.gov/emc/pages/numerical\\_forecast\\_systems/nam.php](https://www.emc.ncep.noaa.gov/emc/pages/numerical_forecast_systems/nam.php). The NCEP NAM 12 km Analysis data was obtained from <https://rda.ucar.edu/datasets/ds609.0/>. From these products, we use potential temperature and 10-m u and v winds for the grid box whose center is located closest to Logan Airport.

### 2.5. Satellite-Based Remote Sensing of NO<sub>2</sub> and Cloud Fraction

Satellite-based remote sensing of atmospheric NO<sub>2</sub> abundance is achieved by optical absorption spectroscopy based on the Beer-Lambert law. Briefly, NO<sub>2</sub> column density (the integrated amount of NO<sub>2</sub> from the surface to the top of the atmosphere, e.g., in molecules cm<sup>-2</sup>) is retrieved by fitting a reference NO<sub>2</sub> absorption spectrum to the measured solar backscatter spectrum (while simultaneously accounting for slowly varying features in the measured spectrum and the impact of other absorbing species) in the neighborhood of 405–430 nm. This fit results in a slant (or “line of sight”) NO<sub>2</sub> column density, which can be converted to a vertical column density using an air mass factor derived from radiative transfer modeling. The tropospheric column densities are inferred by removing an estimate of the stratospheric NO<sub>2</sub> contribution. Here, we make use of the TROPOMI satellite NO<sub>2</sub> retrieval, whose algorithm is documented in van Geffen et al. (2019). The TROPOMI instrument (onboard ESA's Sentinel-5 Precursor) was launched in October 2017 and provides tropospheric NO<sub>2</sub> at a spatial resolution of 3.5 × 5.5 km at nadir (or 7 × 5.5 km prior to August 2019). We grid the individual observations to a regular 0.01° × 0.01° grid using a physics-based oversampling approach provided by Sun et al. (2018), using pixels having a minimum quality assurance value of 0.75, maximum cloud fraction of 0.2, and maximum solar zenith angle of 60°.

We also make use of the cloud fraction retrieval from both the OMI (Vasilkov et al., 2018) and TROPOMI (van Geffen et al., 2019) instruments. Cloud fractions effectively represent the fraction of a pixel that must be covered by a Lambertian reflecting cloud in order to match the measured atmosphere reflectance.

All TROPOMI and OMI data are publicly available and were downloaded from <https://earthdata.nasa.gov/eosdis/daacs/gesdisc>.

### 2.6. Identifying Sea Breezes and Other Predominant Meteorological Conditions

We use the Logan Airport meteorological station to identify sea breeze days and classify other prevailing meteorological conditions. Our analysis is limited to observations made from June, July, and August, since this is the “O<sub>3</sub> season” in the region and since this is when sea breezes tend to occur most frequently in this region (Barbato, 1975). Our algorithm for identifying sea breezes is simple, focusing only on the reversal of winds from systematically westerly in the early morning to systematically easterly during the midday. Other classification schemes may use additional criteria in the identification process and define different types of sea breezes, but to discuss air pollution effects, we expect the reversal of surface winds to be among the most relevant features to identify. Thus, we identify “sea breeze days” as having at least 5 h of westerly (offshore) winds anytime between the hours of 1 a.m. and 12 p.m., followed by at least 5 h of easterly (onshore) winds anytime between the hours of 9 a.m. and 8 p.m. From this definition, we find the average onset time of the sea breeze is 10 a.m. LT (see Section 3.2), but the flexibility of our algorithm allows for the timing of the reversal of wind direction to vary from day-to-day. Judging from the climatological behavior on the population of days that are identified by this algorithm (see in Section 3.2), this simple test successfully selects days with many of the characteristic properties of sea breezes (e.g., clockwise rotation of surface winds, with the offshore-to-onshore transition occurring in the late morning and a maximum onshore wind speed in the middle of the afternoon). We also confirm the quality of this classification by evaluating the vertical profiles of wind and potential temperature, derived from aircraft observations collected at Logan Airport (also discussed in Section 3.2).

The remaining non-sea breeze days were classified as either “westerly prevailing days” (days when the majority of surface winds between the hours of 2 a.m. and 8 p.m. were westerly) or “easterly prevailing days” (days, when the majority of surface winds between the hours of 2 a.m. and 8 p.m., were easterly). Days that did not fall into one of the three above categories were “unclassified,” and made up less than 10% of all days during the period of interest.

## 3. Results

### 3.1. Long-Term Trends in NO<sub>2</sub> and O<sub>3</sub>

We begin with a brief summary of long-term trends in NO<sub>2</sub> and O<sub>3</sub> measured in the Boston region to provide context for the discussion of sea breeze conditions and their importance on local pollutant distribution.

Between 2000 and 2019, summertime midday  $\text{NO}_2$  ground-level concentrations decreased by 60% across all monitoring stations in the Boston area (Figure S1). The steepest absolute declines in  $\text{NO}_2$  concentrations are observed at the most urban and heavily traffic-influenced locations, with a  $-10.4$  ppb/decade trend reported at the Kenmore Square site. The decline in  $\text{NO}_2$  concentrations is consistent with the evidence of large reductions in anthropogenic  $\text{NO}_x$  emissions from urban areas all over the country, which have also been detected by satellite-based observations (e.g., Duncan et al., 2016).

We find that maximum daily ground-level  $\text{O}_3$  concentrations have generally responded to the decline in precursor concentrations (Figure S1). The steepest improvement is found at the predominantly upwind site of Blue Hill, with a decreasing trend of  $-8.0$  ppb/decade, but we find nearly as steep declines at the Lynn and Harbor Island locations. Ozone concentrations at Roxbury, the most urban monitoring location of the four, are suppressed compared to the three other locations. This is explained by the temporary titration of  $\text{O}_3$  (via the  $\text{NO} + \text{O}_3$  reaction to form  $\text{NO}_2$ ) due to high primary  $\text{NO}$  emissions at this urban location. A decrease in this local titration effect over time in response to the decline in  $\text{NO}_x$  emissions could also explain why  $\text{O}_3$  at this site during the last 3 years of this record (2017–2019) were the highest they have been in a decade. There is no statistically significant trend at this location.

We calculate the number of days where maximum daily 8-h  $\text{O}_3$  concentrations exceeded the current guideline concentration established by the EPA of 70 ppb (EPA, 2020). Across the four monitoring sites, the highest number of exceedances in a single summer during this period was observed at the Blue Hill monitoring site in 2003, with a total of 44 days. The Lynn and Harbor Island monitoring sites also experienced their highest number of exceedances that same year (31 and 23 days, respectively). Since then, the number of exceedances has declined substantially, with all three active  $\text{O}_3$  monitoring stations recording fewer than six exceedance days each summer since 2015. While the Boston area is currently in attainment of the National Ambient Air Quality Standard, we note that the  $\text{O}_3$  design values (the 3-year average of the fourth-highest daily maximum 8-h  $\text{O}_3$  concentration, which determines compliance with the standard) at two of the monitoring stations during the 2016–2018 averaging period were 69 and 70 ppb.

We conclude from these long-term observations that the urban Boston region has experienced significant reductions in  $\text{O}_3$  in response to the decline in primary  $\text{NO}_x$  emissions, but that it remains on the cusp of violation of the NAAQS standard, and interannual variability in  $\text{O}_3$  (which is prominent in Figure S1) could be important in maintaining its compliance. With this context, we explore how the sea breeze in this urban area impacts the concentrations of surface  $\text{O}_3$  and its precursors. We choose to focus on observations from 2010 to 2019, to reduce the influence of long-term trends in the data. We further limit our analysis to the stations that have collocated  $\text{NO}_2$  and  $\text{O}_3$  observations (Blue Hill, Roxbury, Harbor Island, and Lynn) so that we are able to neglect the rapid partitioning between  $\text{NO}_2$  and  $\text{O}_3$  in our analysis.

### 3.2. Meteorological Characteristics of Sea Breeze Days and Other Prevailing Conditions

According to our criteria for identifying sea breeze conditions, we find an average of 28.3 sea breeze days (31%) each year between June and August from 2010 to 2019, with considerable interannual variability (Table S1). The highest number of identified sea breeze days was 34 (in 2014) and the minimum was 22 (in 2003). Westerly prevailing conditions are the most frequent in the region, but still only occur an average of 37.4 days (41%) between June and August each year. Easterly prevailing conditions are less frequent than the other two, occurring on average 18.1 days between June and August each year (20%). The remaining days (about 8%) have mixed and unclassified conditions.

Figure 2 shows the climatological mean diurnal evolution of wind conditions observed on days that were identified within each category. Sea breeze days are characterized by mild southwesterly surface winds at the beginning of the day (2–2.5 m/s), which follow the expected clockwise rotation as the day progresses. The surface winds begin to switch from westerly to easterly by mid-morning, with the minimum wind speed observed around 10 a.m., and we interpret this as the average sea breeze “on-set” time. For the following few hours, southeasterly winds persist and gather in strength, achieving a maximum mean wind speed of about 4 m/s by around 4 p.m. LT. Finally, winds continue the clockwise rotation, generally returning to westerly origins by 8:00–9:00 p.m.

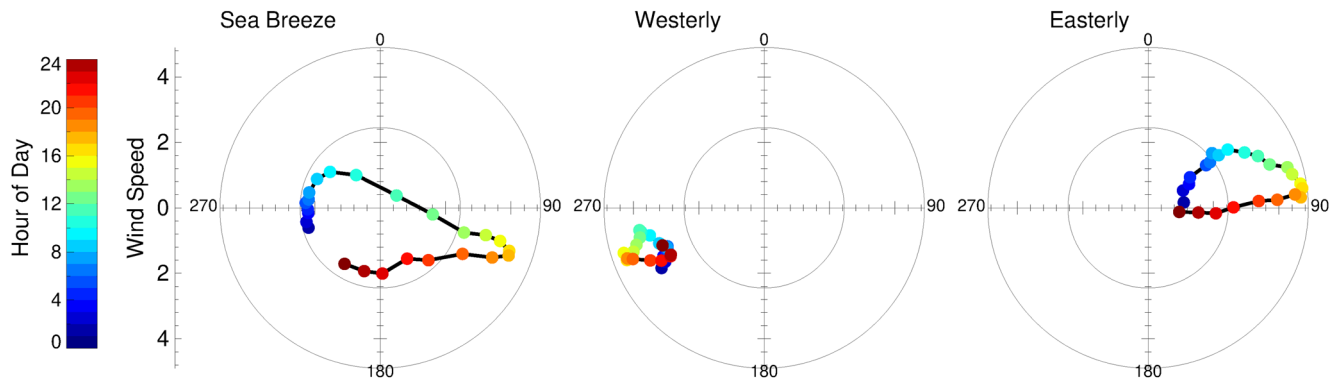
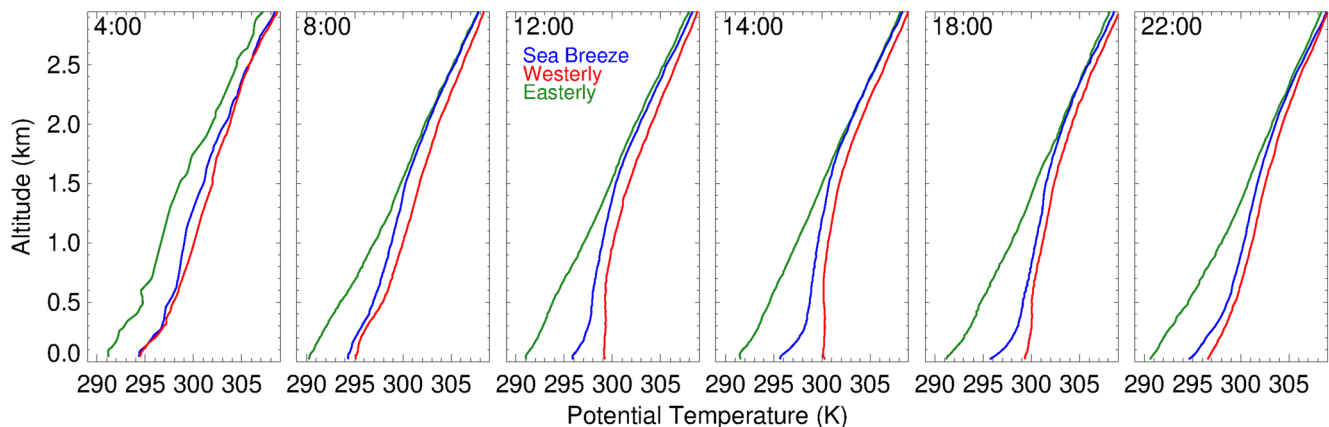


**Figure 2.** Mean wind conditions observed throughout the day at Logan Airport for each predominant meteorological category (June–July–August, 2010–2019).

In contrast, we find that westerly days are characterized by higher surface wind speeds at the beginning of the day (3.5–4 m/s) than on days that result in a sea breeze and change only slightly over the day. The weaker initial wind conditions on sea breeze days may be indicative of high-pressure systems that have been identified as typical during sea breeze development in the region (Barbato, 1975). Easterly prevailing conditions are characterized by the lowest wind speeds at the beginning of the day (~1 m/s), but rise steadily to a maximum in the mid-afternoon (~4.5–5 m/s), corresponding to the time of day that would have the highest temperature contrast between the land and sea.

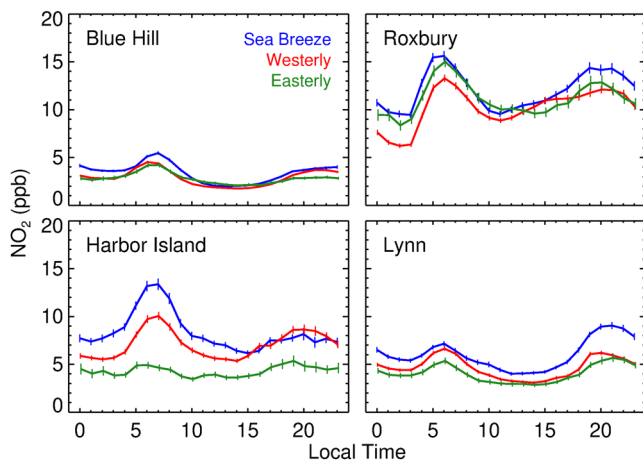
The diurnal evolution of average surface temperatures is likewise characteristic of expectations for each meteorological condition (Figure S2). The coolest days are those with predominantly easterly wind conditions, confirming that relatively cool marine air is being transported inland throughout the day. Surface temperatures during easterly conditions begin around 5–6°C cooler compared to days when the air is coming from the continent, and on average the daily temperatures remain below 20°C. In contrast, surface temperatures on westerly and sea breeze days both begin around 20°C on average. On the westerly days, temperatures continuously rise until about 3:00 p.m. peaking with an average temperature exceeding 28°C. On sea breeze days, temperatures also rise at about the same rate as on westerly days for the first few hours. However, daily maximum temperatures generally occur 2 h earlier on sea breeze days, peaking on average 3–4° cooler than westerly days (with an average of ~24°C by ~12 p.m.). Indeed, the cooler temperatures during sea breezes have the potential to mitigate or eliminate urban heat island effects (He, 2018; He et al., 2020), which have been documented in Boston (Melaas et al., 2016; J. A. Wang et al., 2017).

Figure 3 shows the average vertical profiles of potential temperature derived from aircraft observations at Logan Airport, which provide a climatological perspective of planetary boundary layer evolution during



**Figure 3.** Diurnal evolution of mean vertical potential temperature profiles to 2 km at Logan Airport for each predominant meteorological category (June–July–August, 2010–2019).





**Figure 4.** Diurnal evolution of  $\text{NO}_2$  mixing ratios at the Blue Hill, Roxbury, Harbor Island, and Lynn monitoring stations (June–July–August, 2010–2019). Vertical bars indicate the standard error of the hourly mean.

each prevailing condition. On westerly days, we see evidence typical of the development of a neutral to unstable convective boundary layer that begins forming in the morning and reaches an average depth of around 1–1.5 km by the middle of the afternoon. On easterly days, the atmosphere remains cooler and remarkably stable (i.e., increasing vertical potential temperature profile) throughout all hours of the day. On days that develop a sea breeze, the vertical potential temperature profiles are similar to westerly conditions at the beginning of the day, but by the afternoon we observe a very stable atmosphere near the surface, more consistent with marine atmospheric conditions (with neutral to unstable conditions immediately aloft). Afternoon vertical profiles of u-wind component on sea breeze days (Figure S3) confirm the average height of the sea breeze system is on the order of 300 m.

We use surface meteorological observations at three other locations within and outside of the Boston basin to explore how far the sea breeze may generally penetrate inland (Figure S4). Meteorological observations at the MIT Sailing Pavilion located 6 km west of Logan Airport confirm that the sea breeze usually penetrates at least this far inland. Average wind conditions observed at this location on the days identified as a sea breeze

day based on Logan Airport station data share the same clockwise rotation of wind direction, shifting from westerly to easterly at around 10 a.m. LT and reach a maximum easterly wind speed around 3 p.m. On the other hand, the meteorological observations at the Blue Hill station (18.5 km inland to the southwest) and Hanscom Air Force Base (25 km inland to the northwest) suggest that the sea breeze penetrates this far inland less frequently and that if it does, it arrives much later in the day with weaker winds. These results are consistent with Barbato (1978), which demonstrated that most of the Boston basin sea breeze events are restricted to the first 20 km inland. We note these patterns are highly local and may depend on many climatic and geographic factors such as latitude, sea surface temperature, the shape of the coastline, and regional topographic features. In other coastal areas, sea breezes can also interact with other mesoscale patterns that change their behavior and extent. For example, work on mesoscale circulations in the Mediterranean coast has demonstrated that sea breeze events can be reinforced by anabatic winds caused by the coastal orography mountain ranges (Jiménez et al., 2006; Millán et al., 2002).

Despite being a relatively simple classification system, we find our algorithm results in a convenient and useful grouping of systematic and self-consistent atmospheric conditions, each of which we will show has a statistically distinct impact on air pollutant concentrations and distribution. From this analysis of meteorological observations, we have identified and characterized the following three general atmospheric conditions that prevail in the greater Boston area during the summer: (a) Cool and stable marine atmospheric conditions during consistently easterly days (20%); (b) Warm continental air with the development of a deep convective boundary layer on consistently westerly days (41%); and (c) Sea breeze days that start out with warm but calm westerly conditions, which by the afternoon are characterized by a cool inland breeze at the surface and a very stable atmosphere for the first 300 m above ground level (31%).

### 3.3. Impacts on $\text{NO}_2$ and $\text{O}_3$ Concentrations at the Surface

Figure 4 shows the time-of-day evolution of  $\text{NO}_2$  concentrations at the four monitoring locations where both  $\text{NO}_2$  and  $\text{O}_3$  are available. We first discuss the observations at the Harbor Island site. Given its location in the harbor (Figure 1), we would expect high levels of primary pollution when the winds are coming from the west (since the urban center of Boston is just upwind on those days). When winds are coming from the east, we would expect much lower levels of primary pollution, representative of cleaner marine air. These patterns are evident in the  $\text{NO}_2$  mixing ratios: we see high morning and afternoon peaks during the westerly prevailing days, but essentially no such peaks on the easterly prevailing days. The 24-h average  $\text{NO}_2$  concentrations at this site are 65% higher on westerly days than on easterly days (7.0 vs. 4.3 ppb).

On the days that develop a sea breeze, we find the average morning peak in  $\text{NO}_2$  concentrations at the Harbor Island site is 33% higher than on westerly prevailing days (13.4 vs. 10.0 ppb), despite the fact that both

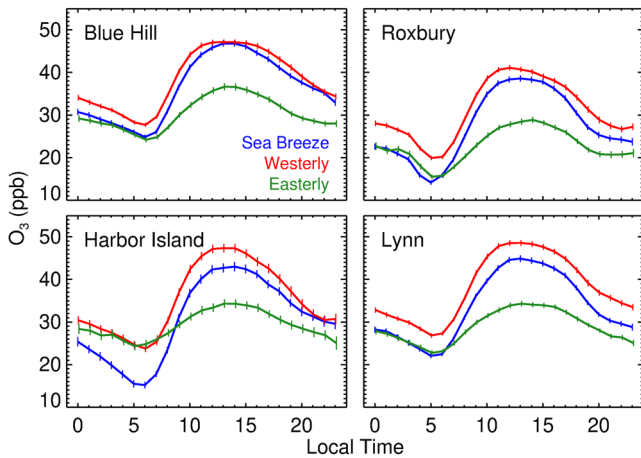


**Figure 5.** Diurnal evolution of  $O_3$  mixing ratios at the Blue Hill, Roxbury, Harbor Island, and Lynn monitoring stations (June–July–August, 2010–2019). Vertical bars indicate the standard error of the hourly mean.

westerly days. The stable atmosphere at this time of day during sea breeze (Figure 3) would also contribute to the enhanced surface concentrations. At the Roxbury and Lynn monitoring stations (which are both located within the topographical basin),  $NO_2$  concentrations on sea breeze days likewise remain higher compared to westerly days for the rest of the day. At Blue Hill, which represents a background location that lies outside of the Boston basin and is not upwind of many  $NO_x$  sources, there is very little difference in  $NO_2$  concentrations between any of the three meteorological conditions.

Figure 5 shows the time-of-day evolution of surface  $O_3$  concentrations at the same four locations. At all four monitoring stations, morning concentrations of  $O_3$  are lower on days that ultimately develop a sea breeze compared to the westerly prevailing days. This can partly be explained by increased titration of  $O_3$  (from the  $NO + O_3$  reaction) due to the higher accumulation of local  $NO_x$  emissions during these mornings discussed above. To account for this local titration effect, we define “Ox” as the sum of  $O_3 + NO_2$  concentrations. Ignoring minor direct emission of  $NO_2$ , Ox accounts for this temporary partitioning so that Ox concentrations will only increase with the chemical production of new  $O_3$ . In this way, Ox provides a more representative depiction of regional net  $O_3$  formation or loss, and also acts as a proxy of secondary pollution from photochemistry. We, therefore, focus on Ox concentrations for the remainder of this analysis.

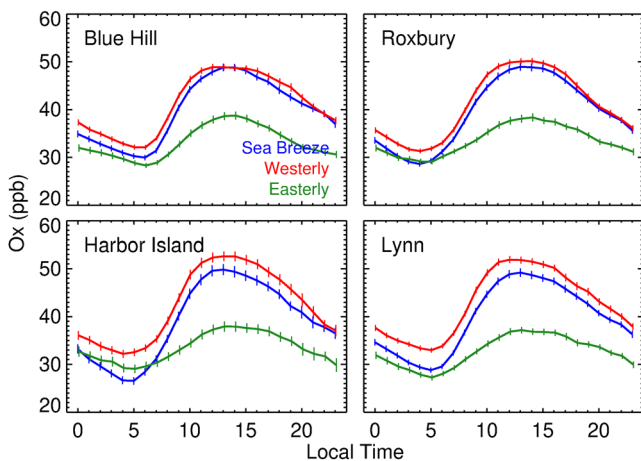


**Figure 6.** Diurnal evolution of Ox mixing ratios at the Blue Hill, Roxbury, Harbor Island, and Lynn monitoring stations (June–July–August, 2010–2019). Vertical bars indicate the standard error of the hourly mean.

are characterized by air being transported from the same direction at this time of day. This implies that sea breeze days are generally characterized by an accumulation of primary emissions at the beginning of the day. We attribute this to the calmer morning horizontal winds, resulting in less ventilation of local morning  $NO_x$  emissions compared to the westerly days with stronger horizontal winds. Since westerly and sea breeze days tend to have similarly stable atmospheric conditions at this time of day (Figure 3), we do not attribute these concentration differences to vertical mixing. We find that on days that develop a sea breeze, the morning  $NO_2$  maxima are enhanced by 6%–16% compared to westerly prevailing days at the other three monitoring locations as well, consistent with calmer morning winds conditions across the region.

In the afternoons (between 12:00 and 3:00 p.m.),  $NO_2$  concentrations at the Harbor Island location remain higher on sea breeze days than on westerly days, despite the winds now coming from the east where there would be negligible primary sources (as demonstrated by the  $NO_2$  concentrations at this time of day during systematically easterly conditions). This confirms that the enhanced local primary pollution from the morning is not only returning inland but tends to remain enhanced relative to

Figure 6 shows the temporal evolution of Ox at each of the monitoring locations. We find Ox concentrations still tend to be lower on the morning of sea breeze days than on westerly days (by 2–6 ppb, depending on location), suggesting that in addition to any enhanced local  $NO$  titration effect, sea breeze days are generally characterized by lower background  $O_3$  levels. In fact, morning Ox concentrations on sea breeze days are similar to the clean easterly days, when the air is consistent of marine origin. This is further evidence that the mornings of sea breeze days are representative of local conditions, with relatively low background secondary pollution compared to westerly days (which, in contrast, would bring background Ox from upwind source regions).

Throughout the late morning (~6–~11 a.m.), the slope of Ox production across the region is about equal on westerly and sea breeze days (3.2–3.9 ppb/h depending on location), implying that chemical  $O_3$  formation during the course of a sea breeze day remains consistent with the production rate of a polluted continental air mass. We find that Ox concentrations during the afternoon sea breeze generally reach the same concentration as on westerly days, to within 2–3 ppb which can largely be accounted for

by the lower background Ox conditions at the beginning of those days. In other words, while background Ox concentrations are lower on sea breeze days, the secondary production of O<sub>3</sub> is as efficient as during westerly days. This result also implies there is little evidence that the cooler average temperatures on sea breeze days mitigate the production of secondary pollution in this urban area. By the afternoon, when the air is returning inland, Ox concentrations are on average 12 ppb higher during sea breeze days than days with systematically easterly winds, further confirming recirculation of continental pollution at the surface. In fact, at the Roxbury monitoring site, located within the basin and the most urban O<sub>3</sub> monitoring location, annual maximum Ox concentrations on sea breeze days were higher than on westerly days for half of the years analyzed (2010, 2012, 2016, 2018, and 2019).

We find that westerly conditions generally contribute disproportionately to the total number of high Ox days in the basin. Of the 50 highest Ox days over the past decade at Roxbury, westerly conditions accounted for almost 70% of them (despite only occurring 40% of the time). Still, sea breeze conditions contribute to all the remaining 30% of the 50 highest Ox days.

In summary, we find that days that develop a sea breeze have relatively low background O<sub>3</sub>, but experience enhanced local primary pollution due to the calm morning conditions. This accumulation of local primary emissions initially contributes to suppressing O<sub>3</sub> concentrations in the morning, but the rate of chemical O<sub>3</sub> production on those days proceeds as it would on days influenced entirely by continental air. Despite the air being transported over the bay and cooling substantially before returning landward, maximum O<sub>3</sub> concentrations during a sea breeze are similar to days when the air is continuously influenced by continental O<sub>3</sub> production and contribute to a substantial fraction of the highest Ox days in the urban area.

### 3.4. Impact on Spatial Variability of Ox at the Surface

The sea breeze also presents the possibility that the physical and chemical properties of air throughout a coastal urban region could exhibit sharp gradients over relatively small horizontal distances (i.e., in the vicinity of the breeze front). From the comparison of meteorological observations at four sites within and outside of the Boston Basin, we inferred that the sea breeze consistently penetrates most of the Boston Basin, but often does not penetrate beyond ~15 km inland. We, therefore, hypothesize that we may see steep contrasts in Ox concentrations across the urban area resulting from air masses with different histories. Such spatial gradients in chemistry have been noted in other examples of urban areas influenced by a sea- or lake-breeze (Blaylock et al., 2017; Castell et al., 2008; Vermeuel et al., 2019; Wentworth et al., 2015). To our knowledge, we are the first to quantify this problem in Boston, and also the first of any sea breeze study to use Ox concentrations, accounting for intra-urban variability in primary NO sources at each location.

We would expect to find gradually increasing Ox concentrations across an upwind-downwind urban transect as O<sub>3</sub> is chemically produced. These gradients within a single urban region would normally be on the order of a few ppb on average since chemical O<sub>3</sub> production can take hours and its atmospheric lifetime near the surface is at least as long (timescales at which air can mix over the entire urban region). Indeed, we observe an increase in peak daytime Ox concentrations on southwesterly dominated days going in the direction from the upwind Blue Hill location, to Roxbury, and ultimately the downwind Lynn location; a similar gradient in the opposite direction is observed on easterly classified days, with peak daytime Ox concentrations increasing in the direction from Lynn, to Roxbury, to Blue Hill (Figure 6).

Larger differences in Ox within a single urban area would not be expected unless the urban area experiences meteorological phenomena that could bring two different air masses with contrasting histories in close proximity, such as would occur at a sea breeze front. Referring to the averaged diurnal profiles in Figure 6, it initially appears as though Ox concentrations are similar across the region during sea breeze conditions (we find that daily maximum average Ox at Blue Hill, Roxbury, and Lynn all reach an average of ~49 ppb). However, this climatological average hides large, but evidently random, variability that is indeed unique and in contrast to the westerly or easterly prevailing days.

We demonstrate this in Figure 7, which shows the temporal evolution of the absolute gradients in Ox concentrations across the Boston basin (Blue Hill - Lynn; and Blue Hill - Roxbury) and within the Boston basin (Roxbury - Harbor Island), according to each prevailing meteorological condition. On sea breeze days, there is a distinct and significant rise in the spatial variability of Ox in the afternoon when compared to the other

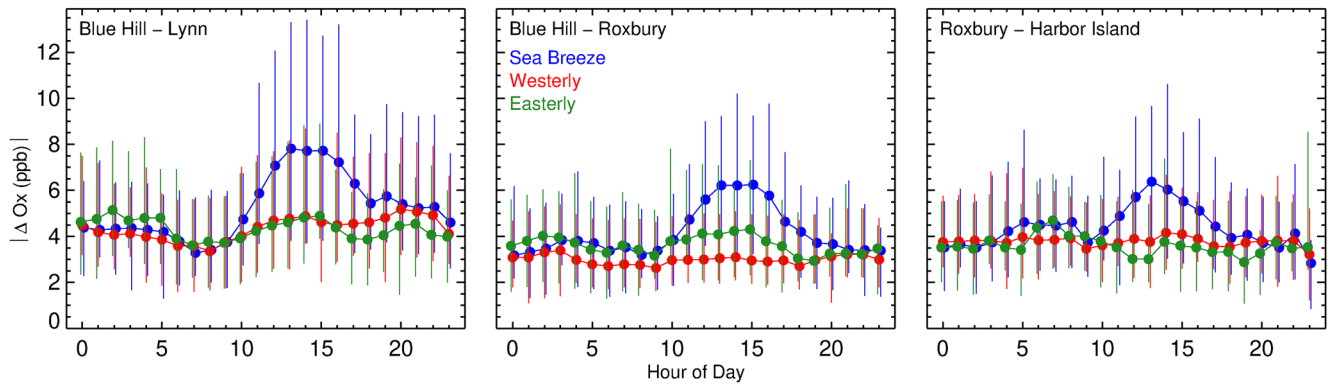


**Figure 7.** Temporal evolution of absolute gradients in Ox concentrations ( $\Delta$  Ox) across and within the Boston basin during each predominant meteorological condition: (top) Blue Hill–Lynn; (middle) Blue Hill–Roxbury; (bottom) Roxbury–Harbor Island. Vertical bars represent the middle 50% of data.

days. While the westerly and easterly prevailing days tend to see Ox gradients on the order of 3–4 ppb, median differences in Ox concentrations across and within the basin on afternoons during a sea breeze are noticeably higher (e.g., 8 ppb between Blue Hill and Lynn; 6 ppb between Blue Hill and Roxbury; and 6 ppb between Roxbury and Harbor Island). The vertical bars in Figure 7 represent the middle 50% of the data, implying that on 25% of days with a sea breeze, differences in afternoon Ox across the basin exceed 13 ppb.

To illustrate this during specific events in detail, Figures 8 and 9 show examples of how the sea breeze drives local spatial variability in Ox, and demonstrate how this gradient can be in any direction. The plots show the hourly timeseries of Ox concentrations (and wind conditions within and outside of the Boston basin) on an example sea breeze day, directly compared to observations during predominantly westerly or easterly conditions during either the immediately preceding or following days. In Figure 8, the period begins with a day of southwesterly flow with consistent Ox concentrations over the whole region as expected (gradients in Ox are only a few ppb). The second day (June 3) is characterized by a strong sea breeze identified by the Logan meteorology, with the reversal of winds occurring around 9 a.m. and maximum easterly winds occurring around 4 p.m. There is likewise a rotation in the winds observed at the Blue Hill site, but these evolve differently over time. We find a gradient in Ox on the order 40 ppb over a distance of only 15 km, persisting for several hours during the midday between Blue Hill and the Harbor Island site. The following day experiences strong easterly conditions which are again characterized by small spatial gradients in Ox.

In Figure 9, this period again begins with a day of strong westerly flow and regionally consistent Ox concentrations. The second day and third day (July 3 and July 4) are characterized by sea breezes identified by the Logan meteorology. From the time the sea breeze is observed at Logan, we find a gradient in Ox on the order of 35 ppb over less than 15 km on July 3, persisting for several hours during the midday between Blue Hill and Roxbury sites. The evolution of surface winds within and outside the Boston basin during the time frame of the sea breeze is demonstrably different, with more southerly (instead of easterly) winds observed at Blue Hill. In this case, the across-basin gradient in Ox is in the opposite direction of the previous example observed in Figure 8, and the winds on July 3 evolve very differently between Logan and Blue Hill. On the other hand, the sea breeze experienced on July 4 is almost experienced identically at Logan and Blue Hill, leading to smaller gradients in Ox than in the other two examples.

We conclude that the sea breeze in Boston does have the capacity to produce steep and often persistent gradients in secondary air pollution (Ox concentration differences that can exceed 30 ppb across less than 15 km), which are not observed on otherwise predominantly westerly or easterly prevailing days. However, these gradients are hidden in the climatological mean since they can be either positive or negative, with evidently roughly equal distribution. We speculate that the true spatial gradients in Ox on any given day are not well captured or resolved by the current monitoring network (which consists of only three active monitoring sites that have collocated NO<sub>2</sub> and O<sub>3</sub> observations). Over the whole metropolitan area of Boston, containing a coastal population of over 4.5 million people and covering an area of around 4,800 km<sup>2</sup>, there are only four currently active monitoring stations that measure collocated NO<sub>2</sub> and O<sub>3</sub> concentrations to allow for an analysis of secondary Ox.

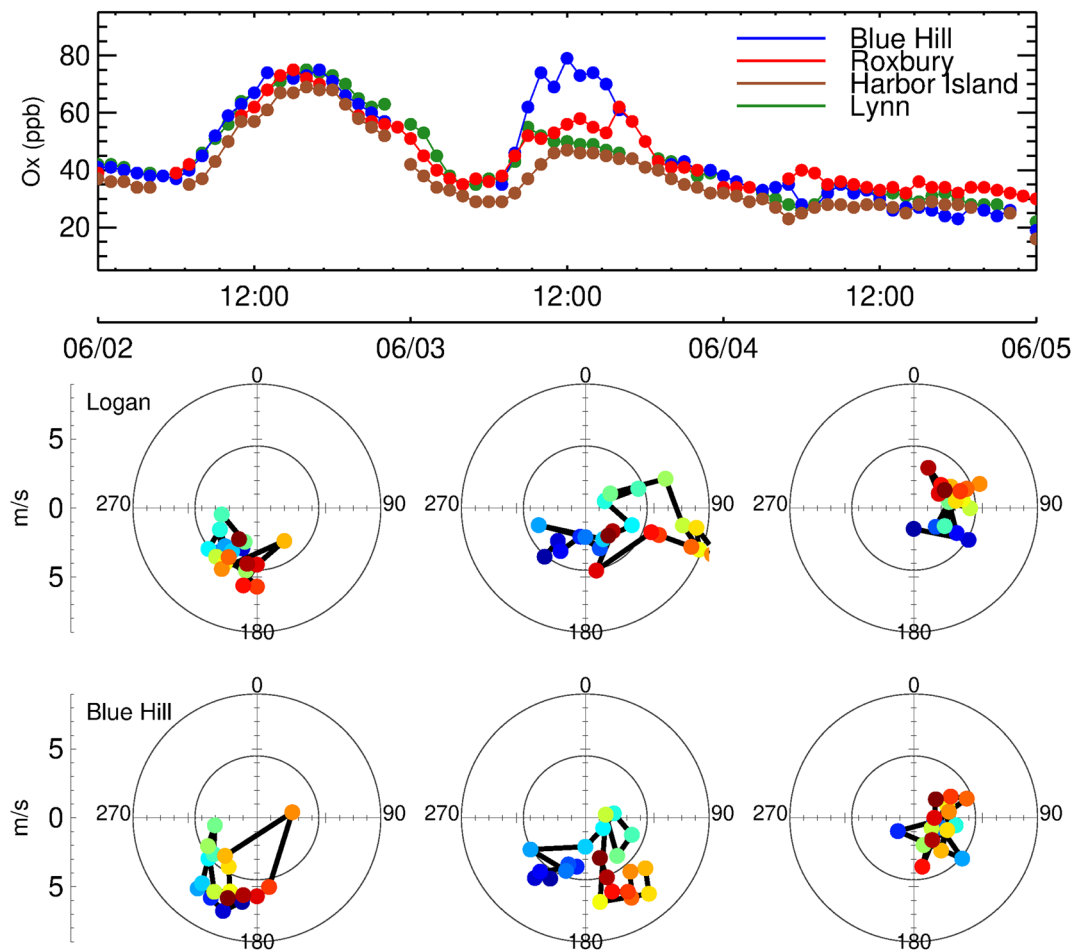


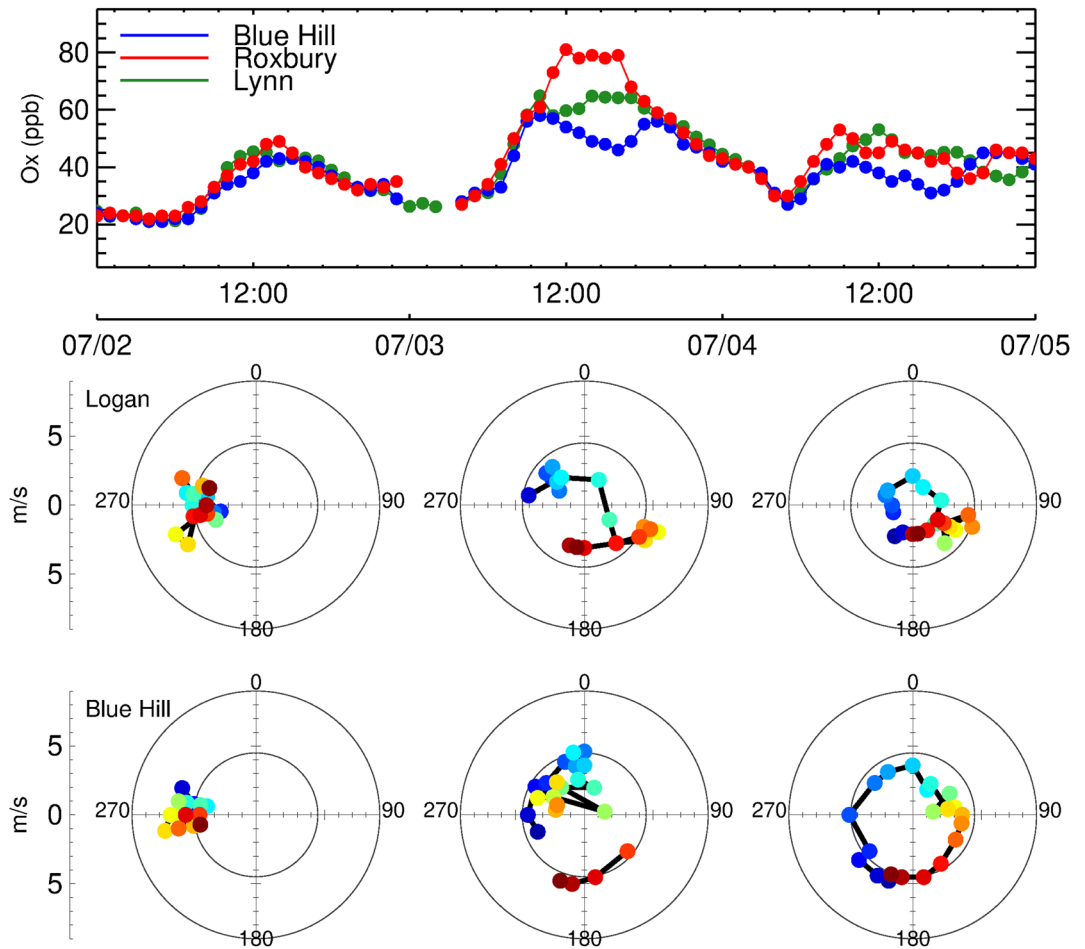
**Figure 8.** Evolution of Ox and surface wind observations across the Boston basin from June 2 to June 5, 2014. The first day is characterized by southwesterly flow, the second day by a characteristic sea breeze leading to steep local gradients in Ox, and the third day by the easterly flow. Color in the wind roses corresponds to an hour of day (shown in Figure 2).

We also speculate that these results may have implications for the spatial distribution of other secondary pollutants that are not regularly monitored. It is widely acknowledged that our ground station monitoring networks fail to capture large heterogeneity in concentrations of primary pollutants such as  $\text{NO}_2$ . Here, we add to the literature showing that steep and persistent gradients in secondary pollution can occur in coastal environments over small spatial scales, which may present an additional monitoring challenge. In the case of Boston, we find that any gradients in potential ambient exposure would tend to average out over the long term. But, this result may be locally specific, and other coastal regions would need to investigate whether more systematic gradients in secondary pollution persist over time during these sea breeze conditions.

### 3.5. Implications for Long-Term Satellite Remote Sensing of Local Air Quality

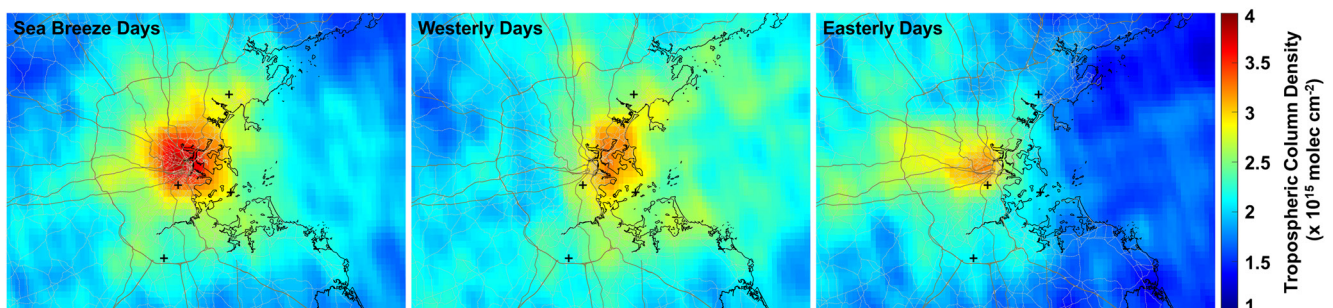
The preceding analysis summarizes how  $\text{NO}_2$  and  $\text{O}_3$  concentrations at the surface evolve during the different prevailing meteorological conditions that occur in the Boston area during the summertime and highlights some implications for representing the spatial distribution of air pollutants in coastal urban environments. Satellite remote sensing observations have the potential to complement sparse ground-based monitoring networks by providing continuous spatial coverage of tropospheric  $\text{NO}_2$  column density.

Figure 10 shows TROPOMI-derived average June-July-August tropospheric  $\text{NO}_2$  column density during sea breeze days compared to the other westerly and easterly prevailing days for the summers of 2018 and 2019. We note that the satellite overpass time is around 1:30 LT, which on sea breeze days lies somewhere



**Figure 9.** Evolution of Ox and surface wind observations across the Boston basin from July 2 to July 5, 2019. The first day is characterized by westerly flow, the second and third day by a characteristic sea breeze leading to steep local gradients in Ox. Color in the wind roses corresponds to an hour of the day (colorbar shown in Figure 2).

between the time of reversal from westerly to easterly winds (~10 a.m. LT) and peak inland wind speeds (~3 p.m. LT). This figure confirms that, when compared with the westerly and easterly prevailing conditions (where local emissions are evidently dispersed in the expected directions), sea breeze days tend to accumulate local NO<sub>x</sub> emissions within the confines of the Boston-area basin. In contrast to in-situ sampling at the surface, remote sensing observations derive the abundance of NO<sub>2</sub> integrated across the atmospheric



**Figure 10.** Satellite-derived tropospheric NO<sub>2</sub> column densities from TROPOMI for June-July-August 2018–2019, averaged separately for each meteorologically prevailing condition. Observations have been gridded from their original pixels to a regular 0.1° × 0.1° grid. The cross symbols indicate the locations of the Blue Hill, Roxbury, Harbor Island, and Lynn monitoring locations.

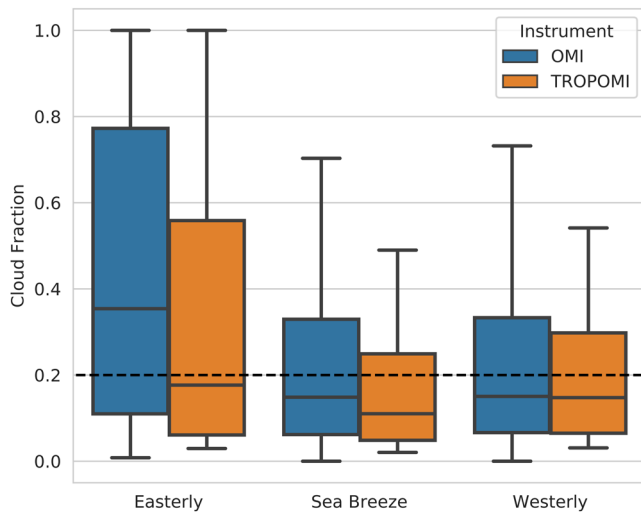


**Figure 11.** Distribution of satellite-derived cloud fraction from the OMI and TROPOMI instruments for easterly, westerly, and sea breeze conditions over Boston. Dashed horizontal line at a cloud fraction of 0.2 represents a typical threshold above which satellite-derived tropospheric column observations are discarded. Boxes encompass the middle 50% of the data (horizontal lines denote the median) and whiskers extend to the 5th and 95th percentiles.

column. Therefore, the satellite measurement alone cannot determine the distribution of  $\text{NO}_2$  with altitude (i.e., whether  $\text{NO}_2$  is only enhanced at the surface, or whether there are other enhancements at altitude with the recirculation). Indeed, the relationship between retrieved tropospheric column from a remote sensing instrument with concentrations near the surface relevant for air quality is a key unknown, and this will be the subject of future modeling investigations. Still, we find maximum tropospheric column density of  $\text{NO}_2$  over the urban area is enhanced by  $\sim 20\%$  on sea breeze days compared to westerly and easterly days. While these satellite-derived maps of  $\text{NO}_2$  tropospheric column density capture the contrasting distribution and movement of urban  $\text{NO}_x$  emissions based on meteorological expectations and surface observations in the Boston basin, their interpretation requires careful consideration.

Here we examine two hypotheses related to some complexities in interpreting satellite-based observations of air quality in this coastal urban environment: (a) we hypothesize that a remote sensing “selection bias” could cause oversampling of some meteorological conditions relative to others due to characteristic cloud conditions and (b) we hypothesize that the horizontal winds that drive chemical transport during sea breeze conditions are not reliably represented in meteorological reanalyses, which could impart higher retrieval error on sea breeze days relative to the other conditions.

To investigate the first hypothesis, Figure 11 shows box plots of the distribution of cloud fractions included with the OMI and TROPOMI satellite products. Generally, a cloud fraction of 0.2 is an acceptable threshold above which the retrieval is subject to large errors in the air mass factor used to convert the “observed” slant column density to a vertical column density (Boersma et al., 2004). The possibility of a “cloud-selection bias” in satellite-derived long-term  $\text{NO}_2$  averages is therefore possible, and has been previously reported in other locations, with different locally dependent mechanisms responsible (e.g., Geddes et al., 2012; McLinden et al., 2014).

In the case of Boston, we see that easterly conditions are generally characterized by a cloudier retrieval than the westerly and sea breeze days. From the OMI product, 61% and 60% of the westerly and sea breeze days respectively have cloud fractions that are below 0.2, but easterly days only have 37% cloud fractions that are below 0.2. Relative to the true frequency of their occurrence, sea breeze, and westerly conditions will therefore get “over represented” in long-term averages of satellite-derived  $\text{NO}_2$  over Boston, while the easterly conditions are relatively under sampled. Indeed, clear skies are one factor that tends to favor the development of sea breezes (Barbato, 1975; Miller, 2003). This implies a potential bias in long-term averages derived from satellite observations (especially relevant for air quality, if column enhancements reflect surface enhancements). Using the TROPOMI product, the fraction of westerly and sea breeze days that are below a cloud fraction of 0.2 is about the same compared to OMI (60% and 63%, respectively). However, the capture of easterly conditions improves dramatically with TROPOMI, such that 56% of easterly days have a cloud fraction below 0.2. This increase in the number of cloud-free observations with better satellite pixel resolution has been predicted in theory (Krijger et al., 2007). Thus, a possible cloud selection bias that might be apparent in OMI becomes less important with TROPOMI observations, despite easterly conditions still having the cloudiest days overall.

The robust statistical sampling of satellite observed  $\text{NO}_2$  during sea breeze conditions relative to their true frequency of occurrence is a notable result, since retrievals during sea breeze conditions may present more difficulties and be prone to additional errors in the retrieval compared to other days. We hypothesize that air mass factor calculations, which account for errors around 30%–60% in tropospheric  $\text{NO}_2$  retrievals over polluted areas (Boersma et al., 2004), will likely suffer from a higher error on sea breeze days than during other more synoptically representative conditions in the region. This is due to the importance of the *a-priori*  $\text{NO}_2$  vertical profile shape used in air mass factor calculations for the retrieval. Accurately representing winds in the *a-priori* models is important for producing correct  $\text{NO}_2$  profile shapes downwind of emissions

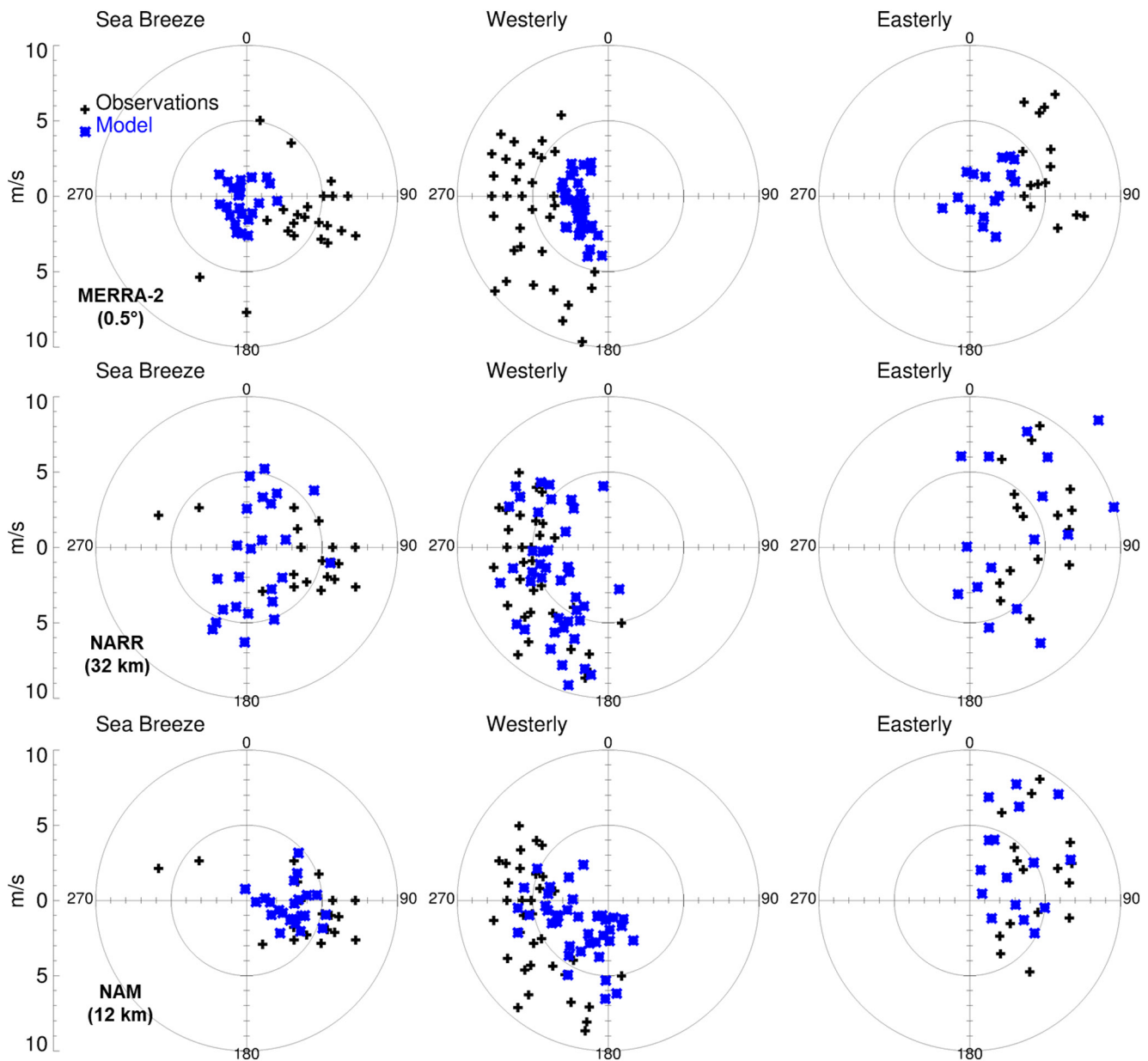


**Figure 12.** Comparing 10-m meteorological reanalysis and analysis results (shown in blue “x”s), with surface observations (shown in black “+”s) divided by prevailing meteorology identified on each day. Top panels show results from MERRA-2 (15:00 LT), middle panels show results from NARR (14:00 LT), bottom panels show results from NAM (14:00 LT). Data are shown for June, July, and August of 2017.

in the urban core. Laughner et al. (2016) demonstrated that the use of daily vertical profile shapes (instead of monthly averaged profiles) substantially impacts retrieved vertical column densities for this reason. In the case of the sea breeze in Boston, we find its spatial extent tends to be smaller than ~20 km, which means that relatively high resolution inputs must be used to accurately predict the transport of NO<sub>x</sub> emissions, and therefore NO<sub>2</sub> vertical profile shapes, during these conditions.

To examine this hypothesis, we compare the winds from three commonly used meteorological products at varying resolutions with the winds measured at Logan Airport. Figure 12 compares the 2 or 3 p.m. LT wind fields obtained from the MERRA-2 (0.5°) and NARR (32 km) meteorological reanalysis products with the observed wind fields for days that were classified as sea breeze, westerly, or easterly predominant conditions during the summer of 2017. These times were chosen given the temporal resolution of the available



products because of their proximity to the TROPOMI overpass time while still being in the afternoon when an inland breeze is most likely to have developed. We note that a coarser MERRA-2 product is used to drive the GMI chemistry-climate model that produces *a-priori* inputs for the NASA standard OMI NO<sub>2</sub> product (Lamsal et al., 2021), while the operational TROPOMI product used in this analysis uses 1° × 1° TM5 global model output driven by ERA-Interim reanalysis meteorological fields (van Geffen et al., 2019; Williams et al., 2017).

Because of their synoptic nature, the westerly and easterly conditions are relatively well represented by both the MERRA-2 and NARR products. While MERRA-2 produces considerably lower wind speeds than observed at Logan airport on these days, the majority of winds occur in the correct quadrants and might be expected to represent NO<sub>2</sub> movement downwind of the urban core reasonably well. However, on days with a sea breeze, both reanalyses have difficulty capturing these conditions at this location; of all sea breeze cases, only 12.5% and 29.2% of winds occur in the correct quadrants for the MERRA-2 and NARR reanalyses respectively. In other words, chemical transport models driven at these resolutions by either reanalysis product would have NO<sub>2</sub> emissions from the urban Boston basin moving in the wrong direction during sea breeze conditions specifically, while more accurately predicting the direction of pollution transport on otherwise systematically westerly or easterly days. Figure 12 also shows the 12 km NAM analysis product compared with observations. We find that this 12 km mesoscale analysis does reproduce the horizontal winds measured at Logan during sea breezes reasonably well (62.5% of the winds in these cases occur in the correct quadrant), suggesting, at least for horizontal transport of near-surface emissions, that a 12 km meteorological input may suffice.

In addition to horizontal mixing of emissions, the vertical profile shape of NO<sub>2</sub> will depend on vertical mixing. We previously showed that vertical mixing conditions within the basin are unique during westerly, easterly, and sea breeze days. We find similar problems with the reanalyzed potential temperature profiles in representing these local conditions (Figure S5). During westerly prevailing days, the evolution of the boundary layer is well represented, producing a well-mixed layer with an average depth of about 1–2 km that is consistent with the aircraft-derived observations at Logan. On the other hand, the potential temperature profiles that are observed at Logan Airport on both sea breeze and easterly prevailing days are not well represented by MERRA-2. Based on the observed potential temperature profiles, we expect sea breezes would be characterized by steep vertical NO<sub>2</sub> gradients due to the strong stability near the surface within the first 300 m in altitude during the sea breeze, with important consequences on the derived air mass factors.

The reanalysis products are not necessarily misrepresenting wind fields at the scale they are meant for; rather, we are highlighting the fact that flow within and across the Boston basin (over which the majority of NO<sub>x</sub> emissions occur) is sufficiently local and complex during sea breezes that these conditions are not correctly represented by reanalyses products commonly used for operational satellite retrievals. Goldberg et al. (2017) also noted this problem in their development of a high-resolution NO<sub>2</sub> retrieval for the Baltimore-Washington metropolitan area. Our results suggest that 12-km resolution inputs for retrievals (e.g., those used in the Berkeley High-Resolution NO<sub>2</sub> retrieval, Laughner et al. [2018]) may at least capture the horizontal winds at the surface accurately in our case. Judd et al. (2019) speculated that higher resolution is needed in some instances of NO<sub>2</sub> retrievals during sea breeze circulations in Los Angeles. Therefore, while the operational TROPOMI retrieval uses daily model inputs, which should improve the retrieval overall compared to using monthly averages, we speculate that a selective systematic error may persist during sea breezes relative to the westerly and easterly prevailing conditions. Future work could examine whether this systematic difference is detectable in ground-based evaluations of the operational versus other retrieval products.

Understanding the implications for capturing the intra-urban differences in NO<sub>2</sub> could benefit from further high-resolution modeling. We note that this issue of misrepresentation due to spatial resolution is not necessarily unique to processes in coastal areas, but the occurrence and important role of the sea breeze in selectively determining pollutant distribution, in this case, exacerbates the challenge. Our results provide additional evidence for the importance of locally or regionally produced research-grade satellite retrievals (Goldberg et al., 2017; Griffin et al., 2019; Laughner et al., 2018), especially for coastal urban environments, driven by high-resolution model inputs over the operational retrievals that use coarse inputs. This happens to be particularly true for Boston, where we find strong sea breeze days are characterized by the highest

accumulation of local emissions, occur around one-third of summer days, and are well-sampled by satellite instruments due to favorable cloud conditions.

Finally, we note that the TROPOMI overpass time does not quite coincide with the average timing of peak sea breeze strength (around 3 p.m.). Future geostationary observations from the TEMPO instrument (expected to launch in 2022) would collect hourly daytime measurements, providing substantially more insight into the temporal evolution of NO<sub>2</sub> if accurate a priori inputs can be acquired. The current generation of satellite-based O<sub>3</sub> retrievals does not provide sensitivity to surface level concentrations to allow a similar investigation, but future observations from TEMPO will benefit from instrumental advantages that should provide insight into boundary layer O<sub>3</sub> variability (Zoogman et al., 2017).

#### 4. Conclusions

We perform a climatological analysis of O<sub>3</sub> and NO<sub>2</sub> observations in the urban Boston area, a region that remains on the cusp of violating national O<sub>3</sub> standards. We specifically characterize the importance of sea breezes in determining the distribution of local atmospheric pollution. We find that sea breeze days, which occur around one-third of the days during summertime in this region, tend to experience low background pollution but an accumulation of local primary emissions and efficient chemical O<sub>3</sub> production so that secondary pollutant concentrations are about as high as on days with consistently polluted continental transport. We add to the literature documenting the presence of steep gradients in secondary pollution in the vicinity of breeze fronts, which pose a challenge to traditional air pollution monitoring networks in coastal urban environments. In the case of Boston, these spatial gradients during sea breezes are masked in the climatological averages.

We note general consistency in the representation of the spatial distribution of local primary emissions in the TROPOMI NO<sub>2</sub> satellite product with meteorological expectations, but confirm hypotheses that may imply challenges in providing accurate long-term averages from these observations. Specifically, there is evidence of a cloud selection bias since sea breeze and westerly conditions tend to be characterized by lower cloud fractions than easterly conditions, although we establish that this bias is improved with an increasing spatial resolution of the satellite footprint. We also show that while winds during synoptic-scale westerly and easterly prevailing days are relatively well represented by common meteorological reanalysis products with spatial resolutions down to ~30 km, the local winds during sea breezes are not. This confirms the challenge in providing a priori chemical inputs that are used in satellite retrievals, which require accurate knowledge of chemical transport, and implies the possibility of a systematic error during sea breeze days compared to westerly or easterly days for pixels over the urban area. These meteorological conditions must be evaluated in the underlying models. This poses a challenge to operational retrieval products given the large number and importance of coastal urban areas around the world. Future work will quantify the magnitude of these potential errors and explore high-resolution modeling and retrieval development. Our observational analysis will be valuable to future high-resolution chemical transport modeling of the region.

#### Acknowledgments

The authors are grateful to the Massachusetts Department of Environmental Protection and to the Environmental Protection Agency for the free and public distribution of air quality monitoring data at <https://www.epa.gov/outdoor-air-quality-data>. The authors also acknowledge the free and public distribution of OMI and TROPOMI satellite products available from the NASA Goddard Earth Sciences Data and Information Services Center at: <https://disc.gsfc.nasa.gov/>. The authors thank the MIT Sailing Pavillion (<http://sailing.mit.edu/weather/>) for access to their meteorological observations upon request. We thank Kang Sun (University at Buffalo) for providing the satellite regridding code publicly. We gratefully acknowledge that this work was funded by a NASA New Investigator Program award to project PI Jeffrey A. Geddes (17-NIP17-0030). The authors also thank the two anonymous reviewers for their constructive feedback.

#### Data Availability Statement

All data used in this analysis are publicly available at the repositories noted in the text. In addition, data used in this analysis is freely available in the Boston University Institutional Repository, OpenBU, at: <https://open.bu.edu/handle/2144/42891>, or by request to the contact author.

#### References

- Angevine, W. M., Senff, C. J., White, A. B., Williams, E. J., Koerner, J., Miller, S. T. K., et al. (2004). Coastal boundary layer influence on pollutant transport in New England. *Journal of Applied Meteorology*, 43(10), 1425–1437. <https://doi.org/10.1175/JAM2148.1>
- Barbato, J. P. (1975). *The sea breeze of the Boston area and its effect on the urban atmosphere*. Boston University.
- Barbato, J. P. (1978). Areal parameters of the sea breeze and its vertical structure in the Boston Basin. *Bulletin of the American Meteorological Society*, 59(11), 2. [https://doi.org/10.1175/1520-0477\(1978\)059<1420:apotsb>2.0.co;2](https://doi.org/10.1175/1520-0477(1978)059<1420:apotsb>2.0.co;2)
- Blaylock, B. K., Horel, J. D., & Crosman, E. T. (2017). Impact of lake breezes on summer ozone concentrations in the Salt Lake valley. *Journal of Applied Meteorology and Climatology*, 56(2), 353–370. <https://doi.org/10.1175/JAMC-D-16-0216.1>
- Boersma, K. F., Eskes, H. J., & Brinkma, E. J. (2004). Error analysis for tropospheric NO<sub>2</sub> retrieval from space. *Journal of Geophysical Research-Atmospheres*, 109(D4), D04311. <https://doi.org/10.1029/2003JD003962>

- Caicedo, V., Rappenglueck, B., Cuchiara, G., Flynn, J., Ferrare, R., Scarino, A. J., et al. (2019). Bay breeze and sea breeze circulation impacts on the planetary boundary layer and air quality from an observed and modeled DISCOVER-AQ Texas case study. *Journal of Geophysical Research: Atmospheres*, *124*(13), 2019JD030523. <https://doi.org/10.1029/2019JD030523>
- Castell, N., Mantilla, E., & Millan, M. (2008). Analysis of tropospheric ozone concentration on a Western Mediterranean site: Castellon (Spain). *Environmental Monitoring and Assessment*, *136*(1–3), 3–11. <https://doi.org/10.1007/S10661-007-9723-1>
- Darby, L. S., McKeen, S. A., Senff, C. J., White, A. B., Banta, R. M., Post, M. J., et al. (2007). Ozone differences between near-coastal and offshore sites in New England: Role of meteorology. *Journal of Geophysical Research*, *112*(D16), D16S91. <https://doi.org/10.1029/2007JD008446>
- Duncan, B. N., Lamsal, L. N., Thompson, A. M., Yoshida, Y., Lu, Z., Streets, D. G., et al. (2016). A space-based, high-resolution view of notable changes in urban NO<sub>x</sub> pollution around the world (2005–2014). *Journal of Geophysical Research: Atmospheres*, *121*(2), 976–996. <https://doi.org/10.1002/2015JD024121>
- Duncan, B. N., Prados, A. I., Lamsal, L. N., Liu, Y., Streets, D. G., Gupta, P., et al. (2014). Satellite data of atmospheric pollution for U.S. air quality applications: Examples of applications, summary of data end-user resources, answers to FAQs, and common mistakes to avoid. *Atmospheric Environment*, *94*, 647–662. <https://doi.org/10.1016/j.atmosenv.2014.05.061>
- Dunlea, E. J., Herndon, S. C., Nelson, D. D., Volkamer, R. M., San Martini, F., Sheehy, P. M., et al. (2007). Evaluation of nitrogen dioxide chemiluminescence monitors in a polluted urban environment. *Atmospheric Chemistry and Physics*, *7*(10), 2691–2704. <https://doi.org/10.5194/acp-7-2691-2007>
- EPA. (2020). *Environmental Protection Agency, Ozone national ambient air quality standards (NAAQS)*. Retrieved from: <https://www.epa.gov/ground-level-ozone-pollution/ozone-national-ambient-air-quality-standards-naaqs>
- Eskes, H., Geffen, J. van, Boersma, F., Eichmann, K.-U., Apituley, A., Padergnana, M., et al. (2020). *Sentinel-5 precursor/TROPOMI level 2 product user manual Nitrogen dioxide*.
- Finardi, S., Agrillo, G., Baraldi, R., Calori, G., Carlucci, P., Ciccioli, P., et al. (2018). Atmospheric dynamics and ozone cycle during sea breeze in a Mediterranean complex urbanized coastal site. *Journal of Applied Meteorology and Climatology*, *57*(5), 1083–1099. <https://doi.org/10.1175/JAMC-D-17-0117.1>
- Geddes, J. A., Murphy, J. G., O'Brien, J. M., & Celarier, E. A. (2012). Biases in long-term NO<sub>2</sub> averages inferred from satellite observations due to cloud selection criteria. *Remote Sensing of Environment*, *124*, 210–216. <https://doi.org/10.1016/j.rse.2012.05.008>
- Gelaro, R., McCarty, W., Suárez, M. J., Todling, R., Molod, A., Takacs, L., et al. (2017). The modern-era retrospective analysis for research and applications, version 2 (MERRA-2). *Journal of Climate*, *30*(14), 5419–5454. <https://doi.org/10.1175/JCLI-D-16-0758.1>
- Goldberg, D. L., Lamsal, L. N., Loughner, C. P., Swartz, W. H., Lu, Z., & Streets, D. G. (2017). A high-resolution and observationally constrained OMI NO<sub>2</sub> satellite retrieval. *Atmospheric Chemistry and Physics*, *17*(18), 11403–11421. <https://doi.org/10.5194/acp-17-11403-2017>
- Goldberg, D. L., Lu, Z., Streets, D. G., De Foy, B., Griffin, D., McLinden, C. A., et al. (2019). Enhanced capabilities of TROPOMI NO<sub>2</sub>: Estimating NO<sub>x</sub> from North American cities and power plants. *Environmental Science and Technology*, *53*(21), 12594–12601. <https://doi.org/10.1021/acs.est.9b04488>
- Griffin, D., Zhao, X., McLinden, C. A., Boersma, F., Bourassa, A., Dammers, E., et al. (2019). High-resolution mapping of nitrogen dioxide with TROPOMI: First results and validation over the Canadian Oil Sands. *Geophysical Research Letters*, *46*(2), 1049–1060. <https://doi.org/10.1029/2018GL081095>
- He, B. J. (2018). Potentials of meteorological characteristics and synoptic conditions to mitigate urban heat island effects. *Urban Climate*, *24*, 26–33. <https://doi.org/10.1016/J.UCLIM.2018.01.004>
- He, B. J., Ding, L., & Prasad, D. (2020). Relationships among local-scale urban morphology, urban ventilation, urban heat island and outdoor thermal comfort under sea breeze influence. *Sustainable Cities and Society*, *60*, 102289. <https://doi.org/10.1016/J.SCS.2020.102289>
- Hwang, M. K., Kim, Y. K., Oh, I. B., Hwa, W. L., & Kim, C. H. (2007). Identification and interpretation of representative ozone distributions in association with the sea breeze from different synoptic winds over the Coastal Urban Area in Korea. *Journal of the Air and Waste Management Association*, *57*(12), 1480–1488. <https://doi.org/10.3155/1047-3289.57.12.1480>
- Janjic, Z. I., Gerrity, J., & Nickovic, S. (2001). An alternative approach to nonhydrostatic modeling. *Monthly Weather Review*. [https://doi.org/10.1175/1520-0493\(2001\)129<1164:AAATNM>2.0.CO;2](https://doi.org/10.1175/1520-0493(2001)129<1164:AAATNM>2.0.CO;2)
- Jiménez, P., Lelieveld, J., & Baldasano, J. M. (2006). Multiscale modeling of air pollutants dynamics in the northwestern Mediterranean basin during a typical summertime episode. *Journal of Geophysical Research: Atmospheres*, *111*(D18), 18306. <https://doi.org/10.1029/2005JD006516>
- Judd, L. M., Al-Saadi, J. A., Janz, S. J., Kowalewski, M. J. G., Bradley Pierce, R., Szykman, J. J., et al. (2019). Evaluating the impact of spatial resolution on tropospheric NO<sub>2</sub> column comparisons within urban areas using high-resolution airborne data. *Atmospheric Measurement Techniques*, *12*(11), 6091–6111. <https://doi.org/10.5194/amt-12-6091-2019>
- Kharol, S. K., Martin, R. V., Philip, S., Boys, B., Lamsal, L. N., Jerrett, M., et al. (2015). Assessment of the magnitude and recent trends in satellite-derived ground-level nitrogen dioxide over North America. *Atmospheric Environment*, *118*, 236–245. <https://doi.org/10.1016/j.atmosenv.2015.08.011>
- Krijger, J. M., van Weele, M., Aben, I., & Frey, R. (2007). Technical Note: The effect of sensor resolution on the number of cloud-free observations from space. *Atmospheric Chemistry and Physics*, *7*(11), 2881–2891. <https://doi.org/10.5194/acp-7-2881-2007>
- Krotkov, N. A., McLinden, C. A., Li, C., Lamsal, L. N., Celarier, E. A., Marchenko, S. V., et al. (2016). Aura OMI observations of regional SO<sub>2</sub> and NO<sub>2</sub> pollution changes from 2005 to 2015. *Atmospheric Chemistry and Physics*, *16*(7), 4605–4629. <https://doi.org/10.5194/acp-16-4605-2016>
- Lamsal, L. N., Krotkov, N. A., Vasilkov, A., Marchenko, S., Qin, W., Fasnacht, Z., et al. (2021). Ozone Monitoring Instrument (OMI) Aura nitrogen dioxide standard product version 4.0 with improved surface and cloud treatments. *Atmospheric Measurement Techniques*, *14*(1), 455–479. <https://doi.org/10.5194/amt-14-455-2021>
- Laughner, J. L., Zare, A., & Cohen, R. C. (2016). Effects of daily meteorology on the interpretation of space-based remote sensing of NO<sub>2</sub>. *Atmospheric Chemistry and Physics*, *16*(23), 15247–15264. <https://doi.org/10.5194/acp-16-15247-2016>
- Laughner, J. L., Zhu, Q., & Cohen, R. C. (2018). The Berkeley high resolution tropospheric NO<sub>2</sub> product. *Earth System Science Data*, *10*(4), 2069–2095. <https://doi.org/10.5194/essd-10-2069-2018>
- Lennartson, G. J., & Schwartz, M. D. (2002). The lake breeze-ground-level ozone connection in eastern Wisconsin: A climatological perspective. *International Journal of Climatology*, *22*(11), 1347–1364. <https://doi.org/10.1002/joc.802>
- Lin, C.-H., Lai, C.-H., Wu, Y.-L., Lin, P.-H., & Lai, H.-C. (2007). Impact of sea breeze air masses laden with ozone on inland surface ozone concentrations: A case study of the northern coast of Taiwan. *Journal of Geophysical Research*, *112*(D14), D14309. <https://doi.org/10.1029/2006JD008123>

- Loughner, C. P., Tzortziou, M., Follette-Cook, M., Pickering, K. E., Goldberg, D., Satam, C., et al. (2014). Impact of bay-breeze circulations on surface air quality and boundary layer export. *Journal of Applied Meteorology and Climatology*, 53(7), 1697–1713. <https://doi.org/10.1175/JAMC-D-13-0323.1>
- Mao, H., & Talbot, R. (2004). Role of meteorological processes in two New England ozone episodes during summer 2001. *Journal of Geophysical Research*, 109(D20), D20305. <https://doi.org/10.1029/2004JD004850>
- Mavrakou, T., Philippopoulos, K., & Deligiorgi, D. (2012). The impact of sea breeze under different synoptic patterns on air pollution within Athens basin. *The Science of the Total Environment*, 433, 31–43. <https://doi.org/10.1016/j.scitotenv.2012.06.011>
- Mazzuca, G. M., Pickering, K. E., New, D. A., Dreessen, J., & Dickerson, R. R. (2019). Impact of bay breeze and thunderstorm circulations on surface ozone at a site along the Chesapeake Bay 2011–2016. *Atmospheric Environment*, 198, 351–365. <https://doi.org/10.1016/j.atmosenv.2018.10.068>
- McLinden, C. A., Fioletov, V., Boersma, K. F., Kharol, S. K., Krotkov, N., Lamsal, L., et al. (2014). Improved satellite retrievals of NO<sub>2</sub> and SO<sub>2</sub> over the Canadian oil sands and comparisons with surface measurements. *Atmospheric Chemistry and Physics*, 14(7), 3637–3656. <https://doi.org/10.5194/acp-14-3637-2014>
- Melaas, E. K., Wang, J. A., Miller, D. L., & Friedl, M. A. (2016). Interactions between urban vegetation and surface urban heat islands: A case study in the Boston metropolitan region. *Environmental Research Letters*, 11(5), 054020. <https://doi.org/10.1088/1748-9326/11/5/054020>
- Mesinger, F., DiMego, G., Kalnay, E., Mitchell, K., Shafran, P. C., Ebisuzaki, W., et al. (2006). North American regional reanalysis. *Bulletin of the American Meteorological Society*, 87(3), 343–360. <https://doi.org/10.1175/BAMS-87-3-343>
- Millán, M., Sanz, M., Salvador, R., & Mantilla, E. (2002). Atmospheric dynamics and ozone cycles related to nitrogen deposition in the western Mediterranean. *Environmental Pollution*, 118(2), 167–186. [https://doi.org/10.1016/S0269-7491\(01\)00311-6](https://doi.org/10.1016/S0269-7491(01)00311-6)
- Miller, S. T. K. (2003). Sea breeze: Structure, forecasting, and impacts. *Reviews of Geophysics*, 41(3), 1011. <https://doi.org/10.1029/2003RG000124>
- NAS. (2016). *The future of atmospheric chemistry research: Remembering Yesterday, understanding Today, Anticipating Tomorrow*: The National Academies Press. <https://doi.org/10.17226/235730>
- NOAA. (2021). *Office for coastal management, Fast facts: Economics and Demographics*. Retrieved from <https://coast.noaa.gov/states/fast-facts/economics-and-demographics.html>
- Reed, A. J., Thompson, A. M., Kollonige, D. E., Martins, D. K., Tzortziou, M. A., Herman, J. R., et al. (2015). Effects of local meteorology and aerosols on ozone and nitrogen dioxide retrievals from OMI and Pandora spectrometers in Maryland, USA during DISCOVER-AQ 2011. *Journal of Atmospheric Chemistry*, 72(3–4), 455–482. <https://doi.org/10.1007/s10874-013-9254-9>
- Russell, A. R., Perring, A. E., Valin, L. C., Bucsel, E. J., Browne, E. C., Min, K.-E., & Cohen, R. C. (2011). A high spatial resolution retrieval of NO<sub>2</sub> column densities from OMI: Method and evaluation. *Atmospheric Chemistry and Physics*, 11(16), 8543–8554. <https://doi.org/10.5194/acp-11-8543-2011>
- Stauffer, R. M., & Thompson, A. M. (2015). Bay breeze climatology at two sites along the Chesapeake bay from 1986–2010: Implications for surface ozone. *Journal of Atmospheric Chemistry*, 72(3–4), 355–372. <https://doi.org/10.1007/s10874-013-9260-y>
- Steinbacher, M., Zellweger, C., Schwarzenbach, B., Bugmann, S., Buchmann, B., Ordóñez, C., et al. (2007). Nitrogen oxide measurements at rural sites in Switzerland: Bias of conventional measurement techniques. *Journal of Geophysical Research: Atmospheres*, 112(D11), D11307. <https://doi.org/10.1029/2006jd007971>
- Sun, K., Zhu, L., Cady-Pereira, K., Chan Miller, C., Chance, K., Clarisse, L., et al. (2018). A physics-based approach to oversample multi-satellite, multispecies observations to a common grid. *Atmospheric Measurement Techniques*, 11(12), 6679–6701. <https://doi.org/10.5194/amt-11-6679-2018>
- Valin, L. C., Russell, A. R., Hudman, R. C., & Cohen, R. C. (2011). Effects of model resolution on the interpretation of satellite NO<sub>2</sub> observations. *Atmospheric Chemistry and Physics*, 11(22), 11647–11655. <https://doi.org/10.5194/acp-11-11647-2011>
- van Geffen, J. H. G. M., Eskes, H. J., Maasakkers, J. D., & Veefkind, J. P. (2019). *TROPOMI ATBD of the total and tropospheric NO<sub>2</sub> data products*. Retrieved from: <https://sentinel.esa.int/documents/247904/2476257/Sentinel-5P-TROPOMI-ATBD-NO2-data-products>
- Vasilkov, A., Yang, E. S., Marchenko, S., Qin, W., Lamsal, L., Joiner, J., et al. (2018). A cloud algorithm based on the O<sub>2</sub>-O<sub>2</sub> 477nm absorption band featuring an advanced spectral fitting method and the use of surface geometry-dependent Lambertian-equivalent reflectivity. *Atmospheric Measurement Techniques*, 11(7), 4093–4107. <https://doi.org/10.5194/amt-11-4093-2018>
- Veefkind, J. P., Aben, I., McMullan, K., Förster, H., de Vries, J., Otter, G., et al. (2012). TROPOMI on the ESA Sentinel-5 Precursor: A GMES mission for global observations of the atmospheric composition for climate, air quality and ozone layer applications. *Remote Sensing of Environment*, 120, 70–83. <https://doi.org/10.1016/j.rse.2011.09.027>
- Vermeuel, M. P., Novak, G. A., Alwe, H. D., Hughes, D. D., Kaleel, R., Dickens, A. F., et al. (2019). Sensitivity of ozone production to NO<sub>x</sub> and VOC along the Lake Michigan coastline. *Journal of Geophysical Research: Atmospheres*, 124(20), 10989–11006. <https://doi.org/10.1029/2019JD030842>
- Wagner, N. L., Riedel, T. P., Roberts, J. M., Thornton, J. A., Angevine, W. M., Williams, E. J., et al. (2012). The sea breeze/land breeze circulation in Los Angeles and its influence on nitryl chloride production in this region. *Journal of Geophysical Research*, 117(D21). <https://doi.org/10.1029/2012JD017810>
- Wang, H., Lyu, X., Guo, H., Wang, Y., Zou, S., Ling, Z., et al. (2018). Ozone pollution around a coastal region of South China Sea: Interaction between marine and continental air. *Atmospheric Chemistry and Physics*, 18(6), 4277–4295. <https://doi.org/10.5194/acp-18-4277-2018>
- Wang, J. A., Hutyrá, L. R., Li, D., & Friedl, M. A. (2017). Gradients of atmospheric temperature and humidity controlled by local urban land-use intensity in Boston. *Journal of Applied Meteorology and Climatology*, 56(4), 817–831. <https://doi.org/10.1175/JAMC-D-16-0325.1>
- Wentworth, G. R., Murphy, J. G., & Sills, D. M. L. (2015). Impact of lake breezes on ozone and nitrogen oxides in the Greater Toronto Area. *Atmospheric Environment*, 109, 52–60. <https://doi.org/10.1016/j.atmosenv.2015.03.002>
- Williams, J. E., Folkert Boersma, K., le Sager, P., & Verstraeten, W. W. (2017). The high-resolution version of TM5-MP for optimized satellite retrievals: Description and validation. *Geoscientific Model Development*, 10(2), 721–750. <https://doi.org/10.5194/GMD-10-721-2017>
- Zhang, L., Zhu, B., Gao, J., & Kang, H. (2017). Impact of Taihu Lake on city ozone in the Yangtze River Delta. *Advances in Atmospheric Sciences*, 34(2), 226–234. <https://doi.org/10.1007/s00376-016-6099-6>
- Zhang, Y., Li, D., Lin, Z., Santanello, J. A., & Gao, Z. (2019). Development and evaluation of a long-term data record of planetary boundary layer profiles from aircraft meteorological reports. *Journal of Geophysical Research: Atmospheres*, 124(4), 2008–2030. <https://doi.org/10.1029/2018JD029529>
- Zoogman, P., Liu, X., Suleiman, R. M., Pennington, W. F., Flittner, D. E., Al-Saadi, J. A., et al. (2017). Tropospheric emissions: Monitoring of pollution (TEMPO). *Journal of Quantitative Spectroscopy and Radiative Transfer*, 186, 17–39. <https://doi.org/10.1016/j.jqsrt.2016.05.008>